The Pharmaceutical and Chemical Journal, 2018, 5(6):29-44

Available online www.tpcj.org

Research Article

ISSN: 2349-7092
CODEN(USA): PCJHBA

Inhibition Properties of Doxycycline for Copper Corrosion in 1M Nitric Acid Solution: Experimental and Quantum Chemical Studies

S. Ouattara, M. A. Tigori, V. Kouakou, P. M. Niamien*, A. Trokourey

Laboratory of Physical Chemistry, Université Félix Houphouët Boigny, Abidjan-Cocody, 22BP 582 Abidjan 22

Abstract Copper corrosion inhibition in 1M nitric acid solution using Doxycycline has been studied by mass loss method and DFT calculations. It was found that this compound acts as a good inhibitor for copper corrosion in the acid solution (the inhibition efficiency is 95.65% at T= 308K and C =10^{-3}M). The inhibiting action of Doxycycline (DXC) was discussed in view of its adsorption on the metal surface. The adsorption was found to be spontaneous and follows the modified Langmuir adsorption isotherm known as Villamil's isotherm. The results show that the inhibition efficiency IE (%) increases with increasing concentration in the studied molecule, but decreases slightly with increasing temperature. The thermodynamic adsorption and activation functions were also determined and discussed. Quantum chemical calculations at B3LYP/6-31G (d) level was further used to determine molecular parameters in order to ascertain any correlation between the inhibition efficiency and the molecular structure.

Keyword: Corrosion inhibition, Mass loss method, DFT calculations, Inhibition efficiency, Molecular descriptors

1. Introduction

Copper and its alloys are among the most used materials in the world. This is due to their excellent electrical and thermal conductivities. They are used in many applications such as electronics devices [1], integrated circuits [2], etc. Though copper is a relatively noble metal, in strongly oxidizing environments, the material is dissolved. This degradation of the material [3- 5] can be controlled by introducing some specific inorganic or organic compounds in the medium. Nowadays, organic inhibitors are preferred to inorganic ones because of increased awareness towards environmental pollution. So [6, 7], only non-toxic and biodegradable compounds are recommended. In the literature the use of many types of compounds such as azoles [8, 9], amines [10, 11], antibiotic drugs [12, 13], etc., is reported. The common feature of these molecules [14, 15] is that they contain heteroatoms such as nitrogen, sulphur, phosphorous and multiple bonds in their structures. Their action depends on the type of functional groups, the number and type of adsorption sites, the charge distribution in the molecule and the type of interaction between these compounds and the metallic surface.

Recently, it has been reported in the literature [16-18] that to get insight into the properties of the organic molecules, quantum chemical calculations were very useful. So, the quantum chemical parameters such as the energy of the highest occupied molecular orbital (E_{HOMO}), the energy of the lowest unoccupied molecular orbital (E_{LUMO}), the energy gap ($\Delta E = E_{LUMO} - E_{HOMO}$), the dipole moment($\mu$), the total energy($E_T$), the absolute electronegativity (χ), the absolute hardness (η), the absolute softness (σ), the fraction of electron transferred (ΔN)and the electrophilicity index (ω) which are the global descriptors related to the interactions between the surface atoms and the organic compounds were correlated to the inhibition efficiency. The local descriptors [19, 20] such as Fukui functions (f_k^+,f_k^-) and the dual descriptor $\Delta f(r) = [f^+(r) - f^-(r)]$were also correlated with the capacity of the molecule to

protect metal surfaces. The global descriptors and the local ones [21] have been reported to be very useful in deriving the inhibition mechanisms.

The aim of the present work is to study the properties of Doxycycline (DXC) as a potential inhibitor of copper corrosion in 1 M nitric acid solution by using mass loss technique and DFT calculations on the electronic parameters. We also intend to establish a relationship between the molecular structure and the inhibition efficiency.

2. Material and methods

2.1 Mass loss technique

The copper samples were of chemical composition in percentage Pb: 0.005, Al: 0.006, Fe: 0.006, S: 0.002 and the remainder Cu: 99.8. Their dimensions were 10mm in length and 2.2 mm in diameter. They were polished with different grade emery papers up to 4/0 grade, cleaned with acetone, washed with doubly distilled water and dried. After being weighed, the samples were introduced in the solution test of 1 M nitric acid in the absence or presence of different concentrations in Doxycycline from Sinopharm Chemical Reagent Co, at different temperatures. The mass loss experiments were performed under total immersion in the test solution, opened to the air. The temperature was controlled by a water thermostat. After one hour immersion, the samples were retrieved from the solution, washed with a bristle brush under running water in order to remove the corrosion product, dried and weighed. The temperature and the concentration range, respectively from 308K to 328K and from 0.05mM to 1 mM. From the weight loss results, the corrosion rates W, the inhibition efficiency IE (%), and the degree of surface coverage θ were calculated using equations (1)-(3):

$$W = \frac{\Delta m}{S \times t} \quad (1)$$

$$IE(\%) = \left(\frac{W_0 - W}{W_0}\right) * 100 \quad (2)$$

$$\theta = \frac{W_0 - W}{W_0} \quad (3)$$

Where Δm is the mass loss (in g), S is the total surface (in cm^2), t is the immersion time (in h), W_0 and W are respectively the corrosion rate without and with the tested molecule and θ is the surface coverage.

2.2 DFT approach

The calculations in this work were performed using the hybrid functional B3LYP, a version of DFT functional that uses Becke's three parameter functional (B3) with a mixture of HF and DFT exchange terms associated with the gradient corrected correlation functional of Lee et al. [22]. The full geometry optimization was carried out at B3LYP/6-31 G(d) level of theory, using Gaussian 03 W [23].

The calculations were carried out in gas phase. The optimized minimum energy geometrical configuration of the molecule is given in Fig 1.

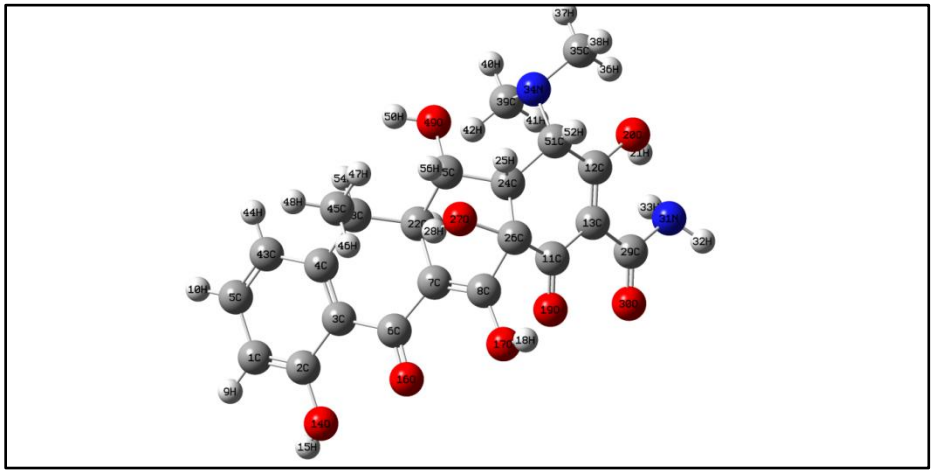

Figure 1: Optimized structure of Doxycycline by 6-31 G (d)

2.2.1 Global descriptors

Electronegativity (χ), chemical potential (μ_P), global hardness (η), global softness (σ) and electrophilicity index (ω) are global reactivity descriptors, highly successful in predicting global chemical reactivity trends.

The chemical potential μ_P [24] is linked with the electronegativity χ via the first derivative of the energy with respect to the number of electrons:

$$\mu_P = \left(\frac{\partial E}{\partial N}\right)_{v(r)} = -\chi \quad (4)$$

In this relation (4), E is the total energy, N is the number of electrons and $v(r)$ is the external potential of the system.

The hardness [25] which is defined as the second derivative of the energy with respect to the number of electrons at $v(r)$ is a property linked to both the stability and the reactivity of the molecule.

$$\eta = \left(\frac{\partial^2 E}{\partial N^2}\right)_{v(r)} \quad (5)$$

Referring to Koopman's theorem [26], the electronegativity (χ) and the global hardness (η) can be written in terms of ionization potential (I) and the chemical affinity (A) or either in terms of HOMO and LUMO energies:

$$\chi = \frac{(I+A)}{2} \approx -\frac{(E_{HOMO} + E_{LUMO})}{2} \quad (6)$$

$$\eta = \frac{(I-A)}{2} \approx -\frac{(E_{HOMO} - E_{LUMO})}{2} \quad (7)$$

The global softness (σ) which is the reciprocal of the global hardness is then given by the equation below:

$$\sigma = \frac{1}{\eta} = \frac{2}{(I-A)} \quad (8)$$

The electrophilicity index (ω) [27], which measures the stabilization in energy when the system acquires an additional electronic charge from the environment is given by the following equation:

$$\omega = \frac{\mu_P^2}{2\eta} = \frac{(I+A)^2}{4(I-A)} \quad (9)$$

Another important quantity linked to the reactivity is the fraction of electron transferred (ΔN) [28], given by:

$$\Delta N = \frac{\phi_{Cu} - \chi_{inh}}{2(\eta_{Cu} + \eta_{inh})} \quad (10)$$

Where ϕ_{Cu} is the copper's work function, η_{Cu} is the copper's hardness, χ_{inh} and η_{inh} are respectively the electronegativity and the hardness of the studied molecule.

For the calculations, the following values have been used: $\phi_{Cu} = 4.52\ eV$ [29] and $\eta_{Cu} = 0$ [30].

2.2.2. Local descriptors

The Fukui functions and the dual descriptor are extensively applied to probe the local reactivity and site selectivity.

The Fukui function [31] is defined as the derivative of the electronic density $\rho(r)$ with respect to the number N of electrons:

$$f(r) = \left(\frac{\partial \rho(r)}{\partial N}\right)_{v(r)} \quad (11)$$

This function reflects the ability of a molecular site to accept or donate electrons. High values of $f(r)$ [31] are associated to a high reactivity at point r. Equation (11) which is associated with a finite difference approximation leads to two definitions of Fukui functions depending on total electronic densities:

$$f^+(r) = \rho_{N+1}(r) - \rho_N(r) \quad (12)$$

$$f^-(r) = \rho_N(r) - \rho_{N-1}(r) \quad (13)$$

In equations (12) and (13), $\rho_{N+1}(r)$, $\rho_N(r)$ and $\rho_{N-1}(r)$ are respectively the densities at point r for the system with $(N+1)$, N and $(N-1)$ electrons.

$f^+(r)$ measures the reactivity at the site r toward nucleophilic attacks, while $f^-(r)$ measures the reactivity at site r towards electrophilic attacks.

Recently, a new descriptor [32, 33] has been introduced. This new index is defined in terms of the variation of hardness with respect to the external potential and is written as the difference between nucleophilic and electrophilic Fukui function, thus been able to characterize both reactive behaviours. This index is given by:

$$\Delta f(r) = [f^{+}(r) - f^{-}(r)] \quad (14)$$

If $\Delta f(r) > 0$, then the site is favoured for nucleophilic attack, whereas if $\Delta f(r) < 0$, the site may be favoured for an electrophilic attack.

3. Results and discussion

3.1 Mass loss method

3.1.1 Effect of concentration

The variation of inhibition the efficiency versus the concentration in DXC for different temperature is shown in Fig. 2. One can observe that the presence of DXC reduces the corrosion of the metal by acting as a physical barrier between copper and its environment. The inhibition efficiency increases with the concentration in DXC: from 75% for 0.05 mM to 95.65% for 1 mM at T = 308K and from 63.8% for 0.05mM to 85.94% to 1 mM at 328K.

3.1.2. Effect of temperature

The evolution of the inhibition efficiency versus the temperature is presented in Fig. 3.

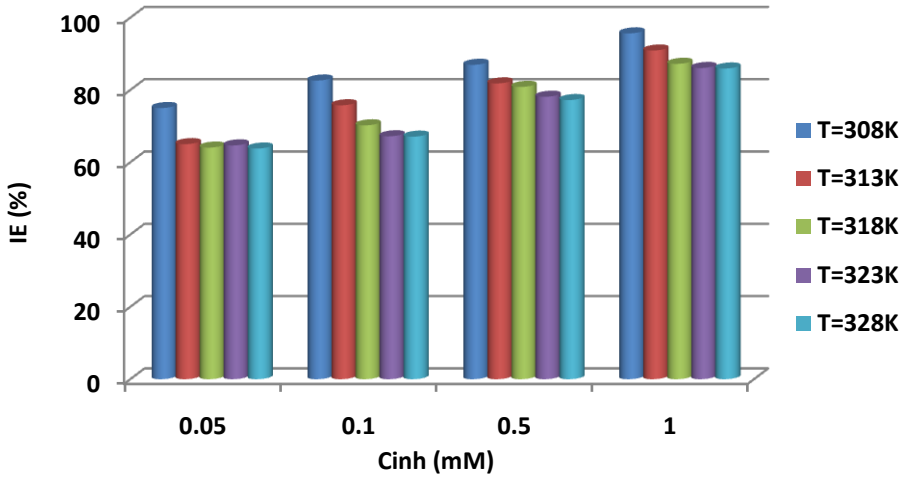

Figure 2: Inhibition efficiency of DXC versus concentration in DXC for different temperature

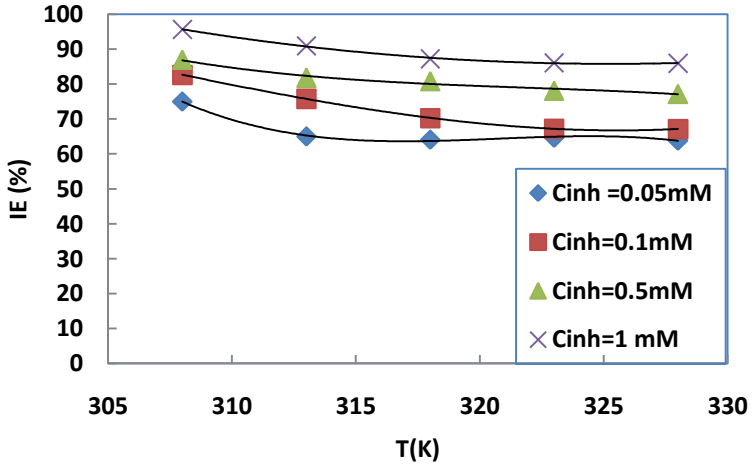

Figure 3: Inhibition efficiency of DXC versus temperature for different concentrations.

It can be seen from Fig. 3 that the inhibition efficiency decreases slightly when the temperature increases, probably due to increase in disorder or to decreasing strength of adsorption (shifting the adsorption-desorption equilibrium towards desorption).

3.2 Adsorption isotherm

In order to understand the interaction between DXC and the copper surface, adsorption isotherm has been used. The values of degree of surface coverage (θ) at different concentrations of DXC in 1M HNO_3 for the temperature range (308-328K) were calculated. Attempts were made to fit (θ) values to various isotherms including, Langmuir, El Awady, Temkin, Freundlich, Flory Huggings. The correlation coefficient (R^2) was then used to choose the best isotherm which was by far the Langmuir isotherm [34]:

$$\frac{C_{inh}}{\theta} = \frac{1}{K_{ads}} + C_{inh} \quad (15)$$

Where K_{ads} is the adsorption equilibrium constant and C_{inh} is the inhibitor concentration. The plots of $\frac{C_{inh}}{\theta}$ versus C_{inh} are given in Fig.4.

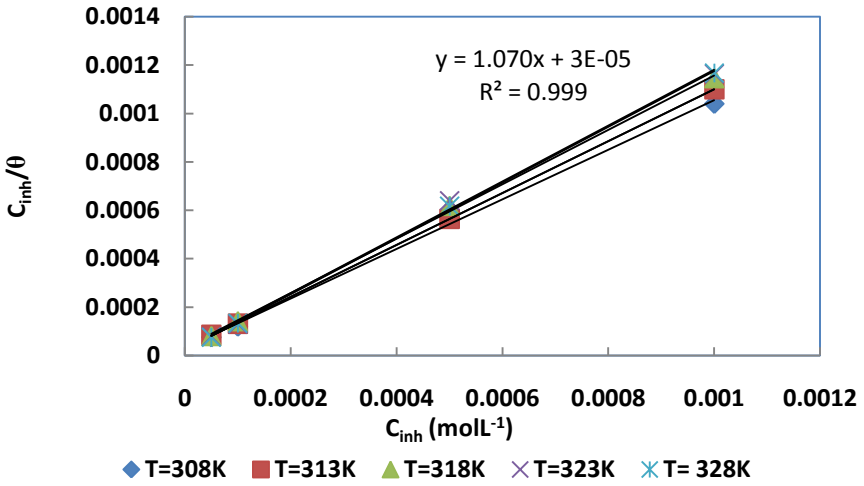

Figure 4: Langmuir isotherm plots for DXC adsorption on copper in 1M HNO_3

Thought the correlation coefficient (R^2) of the Langmuir adsorption isotherm is nearly equal 1, there are deviations from the hypothesis of the model. Therefore, the appropriate isotherm is the modified Langmuir adsorption isotherm named Villamil isotherm [35], which equation is:

$$\frac{C_{inh}}{\theta} = \frac{n}{K_{ads}} + nC_{inh} \quad (16)$$

Where n is the slope value obtained for a plot in Fig. 4.

3.3 Thermodynamic adsorption parameters

Thermodynamic adsorption parameters such as change in the free adsorption enthalpy (ΔG^0_{ads}), change in adsorption enthalpy (ΔH^0_{ads}) and change in adsorption entropy (ΔS^0_{ads})are very important in understanding the mechanism of adsorption process.

The change in free adsorption enthalpy is given by the following equation:

$$\Delta G^0_{ads} = -RT\ Ln\ (55.5K_{ads}) \quad (17)$$

The value of 55.5 is the molar concentration of water in the solution expressed in molarity units (mol.L^{-1}).

The three thermodynamic parameters are linked by the relation below:

$$\Delta G^0_{ads} = \Delta H^0_{ads} - T\Delta S^0_{ads} \quad (18)$$

Fig.5 gives the plot of ΔG^0_{ads} versus T: ΔS^0_{ads} (negative of the slope) and ΔH^0_{ads} (intercept of the line with y axis).

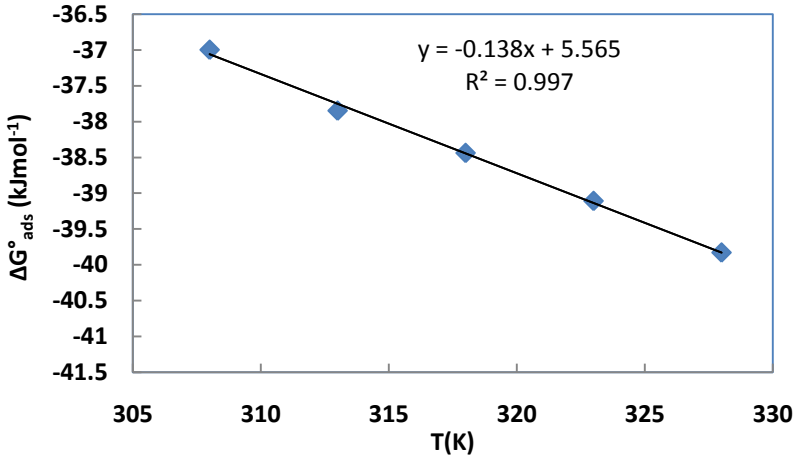

Figure 5: ΔG^0_{ads} versus Temperature for the adsorption of DXC on copper in 1M HNO_3

All the calculated parameters are given in Table 1.

Table 1: Adsorption parameters of DXC on copper surface in 1 M HNO_3

T(K)	$K_{ads}(M^{-1})$	$\Delta G^0_{ads}(kJmol^{-1})$	$\Delta H^0_{ads}(kJmol^{-1})$	$\Delta S^0_{ads}(Jmol^{-1}K^{-1})$
308	34126.7	-37.0		
313	35683.3	-37.8		
318	37433.3	-38.4	5.565	138.4
323	38400.0	-39.1		
328	41379.2	-39.8		

The negative values of ΔG^0_{ads} suggest that the adsorption of DXC on copper surface is a spontaneous process; the values are ranged from -39.8 to -37 kJ.mol^{-1}, indicating [36] that the adsorption process is both physical and chemical adsorption.

The positive value of ΔH^0_{ads} [37] shows that the adsorption of the inhibitor is an endothermic process; this result may explain the fact that the adsorption constant and then the inhibition efficiency increases with increasing temperature.

The change in adsorption entropy ΔS^0_{ads} is positive, showing that disorder increases along the process due probably to the desorption of water molecules.

In order to distinguish between physisorption and chemisorption, the isotherm of Dubinin-Radushkevich [38] has been used. This isotherm is characterized by the equation below:

$$ln\theta = ln\theta_{max} - a\delta^2 \quad (19)$$

Where θ_{max} is the maximum surface coverage and δ is the Polanyi potential which is given by:

$$\delta = RTln\left(1 + \frac{1}{C_{inh}}\right) \quad (20)$$

In equation (20), R is the perfect gas constant, T is the absolute temperature, and C_{inh} is the concentration of the inhibitor expressed in gL^{-1}. The plots of $ln\theta$ versus δ^2 is given in Figure 6.

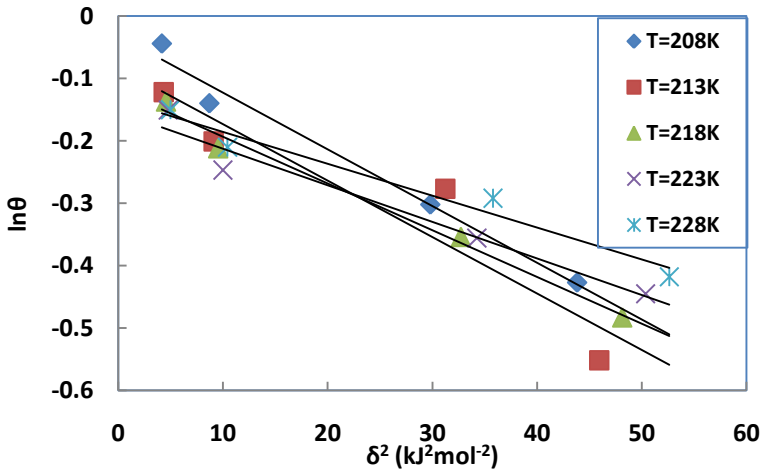

Figure 6: Dubinin-Radushkevich plots for copper corrosion inhibition in presence of DXC

The value of the parameter **a** in equation (19) leads to the mean adsorption energy E_m for the related temperature. This energy which is the transfer energy of 1 mol of adsorbate from the infinity (bulk solution) to the surface of the adsorbent is defined as:

$$E_m = \frac{1}{\sqrt{2a}} \quad (21)$$

All the calculated values are collected in table 2.

Table 2: Parameters of Dubinin-Radushkevich isotherm

T(K)	R^2	$a(kJ^2mol^2)$	θ_{max}	$E_m(kJmol^{-1})$
308	0.983	0.0091	0.969	7.412
313	0.900	0.0090	0.920	7.453
318	0.988	0.0075	0.888	8.165
323	0.956	0.0059	0.857	9.206
328	0.964	0.0051	0.874	9.901

In order to distinguish the range of temperatures for physisorption from that of chemisorption, we plot E_m versus temperature (Figure 7).

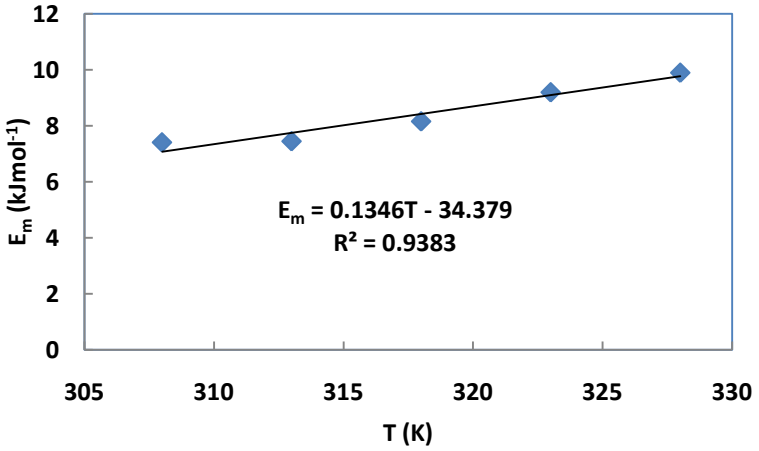

Figure 7: Mean adsorption energy versus temperature for DXC onto copper

The magnitude of E_m [39], gives information about the type of adsorption: E_m values less than 8 kJ mol^{-1} indicate physical adsorption, while that higher than 8 kJ mol^{-1} suggest chemisorption. Using the equation in Figure 7, we

derived the domains where each type of adsorption is predominant ($T < 314.9\ K$ for physisorption and $T > 314.9\ K$ for chemisorption).

3.3 Thermodynamic activation parameters

To study of the effect of the temperature on the corrosion inhibition process, the experiments have been carried out at different temperatures in the absence and presence of various concentration of (DXC). The activation energy for the corrosion process was calculated using the Arrhenius equation:

$$logW = logA - \frac{E_A}{2.303RT} \quad (22)$$

Where W is the corrosion rate, E_a is the apparent activation energy, R is the universal gas constant, T is the absolute temperature and A is the frequency factor.

To access the values of the variations of enthalpy and entropy, the transition state equation has been used:

$$log\left(\frac{W}{T}\right) = log\left(\frac{R}{\aleph h}\right) + \frac{\Delta S_a^*}{2.303\,R} - \frac{\Delta H_a^*}{2.303\,RT} \quad (23)$$

Where $\aleph$ is the Avogadro number, h is the Planck's constant, ΔS_a^* and ΔH_a^* are respectively, the variation of activation entropy and enthalpy.

Figure 8 and 9 display respectively the plots of $logW$ and $log\left(\frac{W}{T}\right)$ versus $\left(\frac{1}{T}\right)$

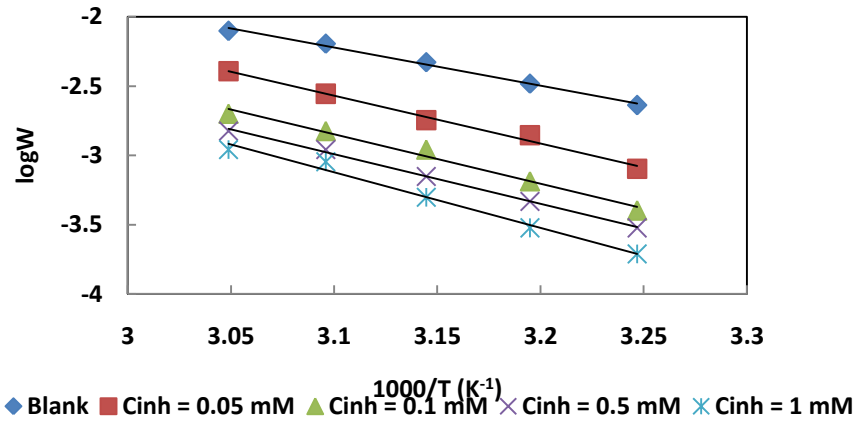

Figure 8: Arrhenius plots for different concentrations of DXC

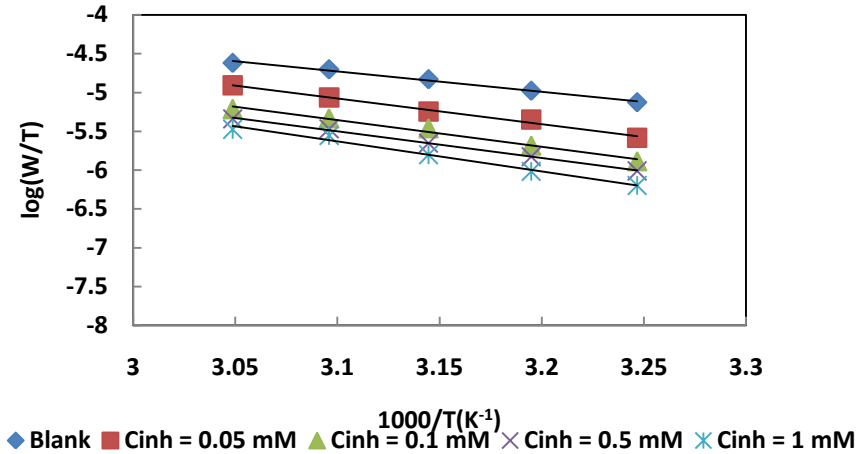

Figure 9: Transition states plots for different concentrations of DXC

The Arrhenius plots of logW against (1/T) gives a straight line with slope ($-\frac{E_a}{2.303R}$) and intercept $logA$; the plots of $log\left(\frac{W}{T}\right)$ versus $\left(\frac{1}{T}\right)$ also give a straight line with slope($-\frac{\Delta H_a^*}{2.303R}$) and intercept of [$log\left(\frac{R}{Nh}\right)+\frac{\Delta S_a^*}{2.303R}$]. The obtained values of the activation parameters are tabulated in Table 3.

Table 3: Activation parameters for copper corrosion without and with DXC in 1 M HNO_3

	E_a (kJmol^{-1})	ΔH_a^* (kJmol^{-1})	ΔS_a^* (Jmol^{-1}K^{-1})
Blank	52.6	50.0	-194.1
0.05 mM	66.1	63.5	-192.3
0.1 mM	68.2	65.6	-192.2
0.5 mM	68.6	65.9	-192.3
1 mM	76.7	74.1	-191.1

The values of E_a for the corrosion process, both in the absence and presence of DXC, are greater than $20kJmol^{-1}$, suggesting [39] that the entire process is controlled by surface reaction. We also note that the values E_a in 1M HNO_3 containing DXC are higher than that in the uninhibited solution, indicating [40] that the adsorption is predominantly physical adsorption (physisorption).

Inspection of data in Table3, also reveal that the activation parameters (ΔH_a^* and ΔS_a^*) of copper dissolution in the presence of DXC are higher than that in the nitric acid solution without the inhibitor. The positive sign of the variation of the activation enthalpy reflects [41] the endothermic nature of copper dissolution, indicating that the dissolution of the metal in presence of DXC is difficult.

The variation of the activation entropy is negative, showing [42] that the rate-determining step for the activated complex is an association rather than dissociation, meaning that a decrease disorder takes place on going from reactants to the activated complex.

3.4 Quantum chemical studies

The calculated molecular parameters, including E_{HOMO} (the energy of the highest occupied molecular orbital), E_{LUMO} (the energy of the lowest unoccupied molecular orbital), the energy gap (ΔE), the dipole momentμ, the electronegativityχ, the hardness η, the softness σ, the electrophilicity index (ω)and the total energy E_T of the molecule are listed in Table 4.

Table 4: Molecular properties of Doxycycline (DXC) calculated by B3LYP/6-31G (d)

Parameter	Value	Parameter	Value
$E_{HOMO}\ (eV)$	-5.662	$\eta(eV)$	1.847
$E_{LUMO}\ (eV)$	-1.968	$\sigma(eV)^{-1}$	0.549
$\Delta E\ (eV)$	3.694	$\mu(D)$	6.809
$I(eV)$	5.662	ΔN	0.191
$A(eV)$	1.968	$\omega(eV)$	3.990
$\chi\ (eV)$	3.815	$E_T(Ha)$	-1564.021

The framework of Density Functional Theory (DFT) [43] is correlated to a number of chemical concepts. Recently, this calculation method [44] has been used to analyse the interactions between organic molecules with heteroatoms and metallic surface in corrosion process.

According to the frontier molecular orbital theory (FMO), chemical reactivity [45] depends on the interaction between HOMO (highest occupied molecular orbital) and LUMO (lowest unoccupied molecular orbital) levels and the reacting species. So, the reactive ability is closely related to the HOMO and LUMO orbitals. Higher E_{HOMO} value means a higher electron-donating ability, while lower E_{LUMO} signifies higher tendency to receive electrons. In our

case, the higher value of E_{HOMO} (-5.662 eV) and the lower value of E_{LUMO} (-1.968 eV) when compared to values in the literature [46, 47], can explain the adsorption on the metallic surface.

The energy gap ($\Delta E = E_{LUMO} - E_{HOMO}$) is an important reactivity parameter. Low value of ΔE signifies better adsorption and higher inhibition efficiency. In our case ($\Delta E = 3.694\ eV$) can be considered [48, 49] as a low value when compared to values in the literature. Figure 10 gives HOMO and LUMO of Doxycycline.

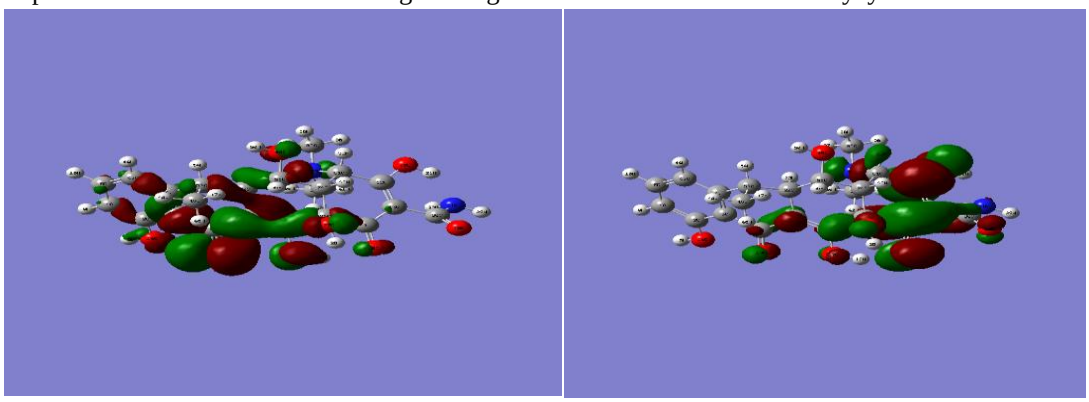

HOMO LUMO

Figure 10: HOMO and LUMO of Doxycycline

The dipole moment μwhich is another important reactivity parameter, results from non-uniform distribution of charges on the different atoms in a molecule. It is the measure of the polarity of a polar covalent bond. In general [50], there is no significant relationship between the dipole moment values and the inhibition efficiency, since some authors [51, 52] state that the lower value of dipole moment favours accumulation of the inhibitor onto the metallic surface, while according to many others [53, 54] the inhibition efficiency increases with increasing values of dipole moment.

The ionization potential (I) and the electronic affinity (A) are another indicators of reactivity; their values are respectively (5.662) and (1.968). This low value of (I) and high value of (A) when compared to values in the literature [39, 55], indicate the capacity of the molecule both to donate and accept electrons.

The molecular stability and reactivity of a molecule is also measured by the absolute hardness (η) and softness (σ). The chemical hardness [56] measured the resistance towards the deformation or polarization of the electron cloud of atoms, ions or molecules, under small perturbation of chemical reaction. DXC has a low hardness value ($\eta = 1.847\ eV$) and high softness value ($\sigma = 0.549$). According to the literature [57, 58], an inhibitor with a low value of hardness and a high value of softness is expected to have high inhibition efficiency, confirming our experimental results.

The positive sign of the number of electrons transferred (ΔN) [59, 60] is an indicator of the tendency of a molecule to donate electrons to the metal. The higher the ΔN value, the greater is the tendency of the molecule to donate electrons to the unfilled orbital of the metal ions (Cu^{2+}: $1s^2 2s^2 2p^6 3s^2 3p^6 d^9$). In our case$\Delta N = 0.191$, showing that DXC can donate electrons to copper ions.

Another important descriptor of reactivity, introduced recently in the literature [61] is the electrophilic index which measures the propensity of chemical species to accept electrons: a high value of electrophilicity index describes a good electrophile, while a small value of electrophilicity indicates a good nucleophile. In our study, $\omega = 3.990\ eV$, shows that the neutral form of DRX has a good capacity to accept electrons from copper.

The total energy calculated by DFT at B3LYP/6-31 G(d) level is also a beneficial parameter. The total energy of a system [62] is the unique functional of charge density. The minimum value of the total energy functional is the ground state energy, giving by the variational principle:

$$E[\rho] = min_n[F(n) + \int d^3 r V_{ext}(r)\rho(r)] \quad (24)$$

Where F[n], $V_{ext}(r)$ and $\rho(r)$ are respectively a universal functional, the external potential and the electronic density. In our study, the total energy of DXC is equal to -1564.021 Hartree, which certainly explain the good inhibition properties observed in experimental data.

Local reactivity of DXC is analysed by means of condensed Fukui functions ($f_k^+ or\ f_k^-$) and the dual descriptor ($\Delta f_k = f_k^+ - f_k^-$), which allow one [63] distinguish each part of the molecule on the basis of its distinct chemical behaviour. The function f_k^+ measures the change of density and it indicates reactivity with respect to nucleophilic attack (when the molecule gains electrons), whereas f_k^- indicates the reactivity with respect to electrophilic attack (when the molecule loss electrons). The dual descriptor [64] is able to correctly predict the site reactivity (most probable nucleophilic or electrophilic attack site). The Fukui functions and dual descriptors of DXC are presented in Table 5.

Table 5: Fukui functions and dual descriptors of DXC

Atom	q_{N+1}	q_N	q_{N-1}	f_k^+	f_k^-	$\Delta f_k = f_k^+ - f_k^-$
1 C	-0.219886	-0.199385	-0.202047	-0.020501	0.002662	-0.023163
2 C	0.323576	0.306452	0.344447	0.017124	-0.037995	0.055119
3 C	0.012171	0.01462	0.009486	-0.002449	0.005134	-0.007583
4 C	0.048709	0.115134	0.053714	-0.066425	0.06142	-0.127845
5 C	-0.136315	-0.124967	-0.117653	-0.011348	-0.007314	-0.004034
6 C	0.347697	0.34885	0.386343	-0.001153	-0.037493	0.03634
7 C	-0.186745	0.023322	-0.122224	-0.210067	**0.145546**	**-0.355613**
8 C	0.362797	0.306405	0.362776	0.056392	-0.056371	0.112763
9 H	0.095822	0.116182	0.161441	-0.02036	-0.045259	0.024899
10 H	0.106431	0.132043	0.173407	-0.025612	-0.041364	0.015752
11 C	0.346688	0.394501	0.405936	-0.047813	-0.011435	-0.036378
12 C	0.244663	0.329758	0.28778	-0.085095	0.041978	-0.127073
13 C	0.009885	-0.056696	0.028587	0.066581	-0.085283	0.151864
14 O	-0.62354	-0.605312	-0.619198	-0.018228	0.013886	-0.032114
15 H	0.386634	0.403965	0.420229	-0.017331	-0.016264	-0.001067
16 O	-0.522634	-0.461233	-0.414164	-0.061401	-0.047069	-0.014332
17 O	-0.582082	-0.613698	-0.516097	0.031616	-0.097601	0.129217
18 H	0.375367	0.433493	0.443151	-0.058126	-0.009658	-0.048468
19 O	-0.483509	-0.526899	-0.34852	0.04339	-0.178379	0.221769
20 O	-0.635445	-0.601904	-0.593332	-0.033541	-0.008572	-0.024969
21 H	0.393819	0.44035	0.425674	-0.046531	0.014676	-0.061207
22 C	-0.291786	-0.173988	-0.31763	-0.117798	0.143642	-0.26144
23 H	0.166166	0.171591	0.232869	-0.005425	-0.061278	0.055853
24 C	-0.147853	-0.168724	-0.178773	0.020871	0.010049	0.010822
25 H	0.184505	0.166754	0.248098	0.017751	-0.081344	0.099095
26 C	-0.03755	0.129871	0.037155	-0.167421	0.092716	-0.260137
27 O	-0.656356	-0.618198	-0.548842	-0.038158	-0.069356	0.031198
28 H	0.519345	0.404983	0.54341	**0.114362**	-0.138427	**0.252789**
29 C	0.440862	0.50649	0.49524	-0.065628	0.01125	-0.076878
30 O	-0.434316	-0.427238	-0.389806	-0.007078	-0.037432	0.030354
31 N	-0.800788	-0.791584	-0.801691	-0.009204	0.010107	-0.019311
32 H	0.321395	0.349313	0.378158	-0.027918	-0.028845	0.000927
33 H	0.323981	0.349282	0.359148	-0.025301	-0.009866	-0.015435
34 N	-0.365779	-0.367762	-0.347634	0.001983	-0.020128	0.022111

35	C	-0.316408	-0.31007	-0.353867	-0.006338	0.043797	-0.050135
36	H	0.196258	0.138828	0.234105	0.05743	-0.095277	0.152707
37	H	0.103808	0.152358	0.17364	-0.04855	-0.021282	-0.027268
38	H	0.110093	0.170468	0.166486	-0.060375	0.003982	-0.064357
39	C	-0.305813	-0.321147	-0.338456	0.015334	0.017309	-0.001975
40	H	0.096581	0.167085	0.17788	-0.070504	-0.010795	-0.059709
41	H	0.062093	0.108405	0.114564	-0.046312	-0.006159	-0.040153
42	H	0.236639	0.174011	0.224676	0.062628	-0.050665	0.113293
43	C	-0.170684	-0.204628	-0.167249	0.033944	-0.037379	0.071323
44	H	0.104419	0.118704	0.147389	-0.014285	-0.028685	0.0144
45	C	-0.452943	-0.449099	-0.474034	-0.003844	0.024935	-0.028779
46	H	0.184724	0.171126	0.192236	0.013598	-0.02111	0.034708
47	H	0.156024	0.143665	0.168041	0.012359	-0.024376	0.036735
48	H	0.126422	0.150188	0.203703	-0.023766	-0.053515	0.029749
49	O	-0.677762	-0.656601	-0.625253	-0.021161	-0.031348	0.010187
50	H	0.35465	0.400664	0.420238	-0.046014	-0.019574	-0.02644
51	C	-0.074472	-0.040343	-0.078517	-0.034129	0.038174	-0.072303
52	H	0.147365	0.193996	0.217886	-0.046631	-0.02389	-0.022741
53	C	-0.168661	-0.193515	-0.198267	0.024854	0.004752	0.020102
54	H	0.10479	0.106504	0.152755	-0.001714	-0.046251	0.044537
55	C	0.104321	0.125719	0.092137	-0.021398	0.033582	-0.05498
56	H	0.192625	0.147911	0.270468	0.044714	-0.122557	0.167271

The results reported in Table 5 reveal that most probable site for nucleophilic attack (site of highest value of f_k^+) is H (28) atom in the LUMO region. The electrophilic attack site (site of highest value of f_k^-) is C (7) atom in the HOMO region. These results are supported by the values of the dual descriptor Δf.

3.5 Corrosion inhibition mechanism

The experimental results show that:

- DXC can give electrons to copper ($\Delta N = 0.191$) (chemisorption)
- DXC can receive electrons from copper via Cu^{2+} ($\omega = 3.99\ eV$) (chemisorption)
- In HNO_3, DXC is protonated: $DXC + H^+ \rightarrow [DXCH]^+$

$[DXCH]^+$ interact (electrostatic interaction) with NO_3^- adsorbed on the metallic surface covered by Cu^{2+}.

The proposed schematic interaction mechanism is given by Figure 11.

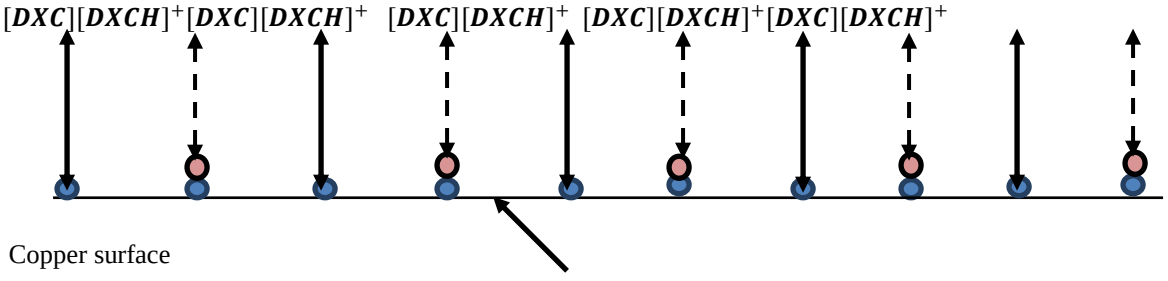

Figure 11: Schematic mechanism of copper corrosion inhibition by DXC

: Cu^{2+} ion : NO^{3-} ion ⟷ : chemisorption ←– –→ : physisorption

4. Conclusion

Doxycycline acts as a good inhibitor for copper corrosion in 1.0M HNO_3. The inhibition efficiency increases with increasing concentration of DXC, but decreases when temperature rises. The adsorption of DXC onto copper obeys the Villamil isotherm. The thermodynamic functions of adsorption and activation reveal a spontaneous adsorption and indicate both type of adsorption (physisorption and chemisorption). The quantum chemical calculations support experimental results.

Conflicts of interest

The authors declare that they have no conflicts of interest.

References

1. Otieno-Alego V., Huynh N., Natoya T., Bottle S. E., & Schweinsberg D. P. (1999). Inhibitive effect of 4- and (-carboxylbenzotriazole on copper corrosion in acidic sulphate and hydrogen sulphide solutions. *Corros. Sci*. 41(4), 685-697.
2. Tsai H. Y., Sun S. C., & Wang S. J. (2000). Characterization of Sputtered Tantalum Carbide Barrier Layer for copper Metallisation. *J. Electrochem. Soc*. 147(7), 2766-2772.
3. Igual Munoz A., Garcia Anton J., Guinon J. L., & Perez Herranz V. (2004). Comparison of inorganic inhibitors of copper, nickel and copper-nickels in aqueous lithium bromide solutions. *Electrochemica Acta* 50(4), 957-966.
4. Sherif E. M., & Park S. M. (2005). Inhibition of copper inhibition in 3% NaCl solution by N-phenyl-1,4-phenylenediamine. *J. Electrochem Soc*. 152(10), 3428-3433.
5. Falluvena T., Antonow M., & Goncalves R. S. (2006). Caffeine as non-toxic corrosion inhibitor for copper in aqueous solutions of potassium nitrate. *Appl. Surf. Sci*. 253(2), 566-571.
6. Simonovic A. T., Petrovic M.B., Radonavovic M. B., Milik S. M., & Antonijevic M. M. (2014). Inhibition of copper corrosion in acid sulphate media by eco-friendly amino acid compound. *Slovak Academy of Sciences* 68(3), 1-10.
7. Mobin M., Aslam R., & Aslam J. (2017). Non-toxic biodegradable cationic Gemini surfactants as novel corrosion inhibitor for mild steel in sodium salicylate: Experimental and theoretical approach. *Materials Chemistry and Physics* 191, 151-167.
8. Zhao Y. S., Yang W., Zhang G., Ma Y., & Yao J. (2006). A hierarchical self-assembly of 4,5-diphenylimidazole on copper. *Colloids and Surfaces A: Physicochem. Eng. Aspects* 277(1-3), 111-118.
9. Lalitha A., Ramesh S., & Rajeswari S. (2005). Surface protection of copper in acid medium by azoles and surfactants. *Electrochimica Acta* 51(1), 47-55.
10. Sherif E. M., & Park S. M. (2006). Inhibition of copper in acidic pickling solutions by N-phenyl-1, 4-phenylenediamine. *Electrochimica Acta* 51(22), 4665-4673.
11. Ehteshamzade M., Shahrabi T., & Hosseini M. G. (2006). Inhibition of copper corrosion by self-assembled films of new Schiff bases and their modification with alkanethiols in aqueous medium. *Applied Surface Science* 252 (8), 2949-2959.
12. Ade S. B., Shitole N. V., & Lonkar S. M. (2014). Antibiotic drugs used as metal corrosion inhibitor in various acid medium. *Journal of Chemical and Pharmaceutical Research* 6, 1865-1872.
13. Fouda A. S., & Gadow H. E. (2014). Streptoquin and Septazole Antibiotic drugs as corrosion inhibitors for copper in aqueous solutions. *Global Journal of Researches in Engineering: C Chemical Engineering*. 14, 21-36.
14. Belpour M., Ghoreishi S. M., Niasari M. S., & Ebrahimi B. (2008). Evaluating two new synthesized S-N Schiff bases on the corrosion of copper in 15% hydrochloric acid. *Mater. Chem. Phys*. 107, 153-157.
15. Khaled K. F. (2008).Adsorption and inhibitive properties of a new synthesized guanidine derivative on corrosion of copper in 0.5M H_2SO_4. *Appl. Surf. Sci*. 255, 1811-1818.

16. Aouniti A., Khaled K. F., & Hammouti B. (2013). Correlation between inhibition efficiency and chemical structure of some amino acids on the corrosion of Armco Iron in Molar HCl. *Int. J. Electrochem. Sci*. 8, 5925-5943.
17. Demissie E. G., Kassa S. B., & Woyessa G. W. (2014). Quantum chemical study on corrosion inhibition efficiency of 4-amino-5-mercapto-1, 2, 4-triazole derivatives for copper in HCl solution. *International Journal of Scientific Research*. 5(6), 304-312.
18. Efil K., & Obot I. B. (2017). Quantum chemical investigation of the relationship between molecular structure and corrosion inhibition efficiency of Benzotriazole and its alkyl- derivatives on Iron. *Protection of Metals and Physical Chemistry of Surfaces*. 53(6), 1139-1149.
19. Olah J., & Van Alsenoy C. (2002). Condensed Fukui Functions derived from Stockholder charges: Assessment of their performance as local reactivity descriptors. *Journal of PhysicalChemistry* A. 106 (15), 3885-3890.
20. Morell C., Grand A., & Torro Labbé A. (2006). Theoretical support for using $\Delta f(r)$ descriptor. *Chem. Phys. Lett*. 425, 342-346.
21. Olasunkanmi L. O., Kabanda M.M., & Ebenso E. E. (2016). Quinoxaline derivatives as corrosion inhibitors for mild steel in hydrochloric acid medium: Electrochemical and quantum chemical studies. *Physica E*76, 109-126.
22. Lee C., Yang W., & Parr R. G. (1988). Development of the Colle-Salvetti correlation-energy formula into a functional of the electron density. *Physical Review B: Condensed Matter and Materials Physics*. 37(2), 785-789.
23. Frisch M. J., Trucks G. W., Schlegel H. B. et al. (2003). *Gaussian Inc*., Pittsburgh, Penn, USA.
24. Parr R. G., Donnelly R. A., Levy M., & Palke W. E. (1978). *J. Chem. Phys*. 68(8), 3801-3807.
25. Parr R. G., & Pearson R. G. (1983). Absolute hardness: companion parameter to absolute electronegativity. *J. Am Chem. Soc*. 105 (26), 7512-7516.
26. Koopmans T. (1934). Über die zuordnung von wellenfunktionnen und Eigenwerten zu den einzelnen Elektronen eines Atoms. *Physica*. Elsevier 1(1-6), 104-113.
27. Parr R. G., Szentpaly L., & Liu S. (1999). Electrophilicity index. *J. Am Chem. Soc*. 121 (9), 1922-1924.
28. Kokalj A., & Kovacevic N. (2011). On the consistent use of electrophilicity index and HSAB-based electron transfer and its associated change of energy parameters. *Chem. Phys. Lett*. 507 (1-3), 181-184.
29. Nieuwenhuys B. E., Van Aardenne O. G., & Sachter W. M. H. (1974). *Chem. Phys*. 5(3), 418-428.
30. Sastri V. S., & Perumarddi J.R. (1997). Molecular orbital theoretical studies of some organic corrosion inhibitors. *Corrosion*. 53(8), 617-622.
31. Geerlings P., De Proft F., & Langenaeker W. (2003). Conceptual Density Functional Theory. *Chem. Rev*. 103(5), 1793-1874.
32. Morell C., Grand A., & Torro Labbé A. (2005). New Dual Descriptor for Chemical Reactivity. *J. Phys. Chem. A*. 109 (1), 205-212.
33. Morell C., Grand A., & Torro Labbé A. (2006). Theoretical support for using Δf(r) descriptor. *Chem. Phys. Lett*. 425 (4-6), 342-346.
34. Li X. H., Deng S. D., Mu G. N., Fu H., & Yang F. (2008). Inhibition effect of non-ionic surfactant on the corrosion of cold rolled steel in hydrochloric acid. Corros. Sci.50 (2), 420-430.
35. Villamil R. F. V., Corio P., Agostinho S. M. L., & Rubin J. C. (1999). Effect of sodium dodecylsulfate on copper corrosion in sulphuric acid media in the absence and presence of benzotriazole. Journal of Electroanalytical Chemistry, 472 (2), 112-119.
36. Moretti G., Guidi F., & Grion G. (2004). Tryptamine as a green iron corrosion inhibitor in 0.5M sulphuric acid. Corrosion Science, 46 (2), 387-403.
37. Durnie W., Marco R. D., Jefferson A., & Kusella B. (1999). Development of a structure-activity relationship for oil field corrosion inhibitors. J. Electrochem. Soc. 146, 1751-1756.

38. NoorE. A. (2009). Potential of aqueous extract of Hibiscus sabdariffa leaves for inhibiting the corrosion of aluminium in alkaline solutions. Journal of Applied Electrochemistry, 39 (9), 1465-1475.
39. Obi-EgbediN. O., & ObotI. B. (2011). Inhibitive properties, thermodynamic and quantum chemical studies of alloxazine on mild steel corrosion in H_2SO_4, Corros. Sci. 53, 263-275.
40. Tang Y., Zhang F., Hu S., Cao Z., Wu Z., & W Jing. (2013). Novel benzimidazole derivatives as corrosion inhibitors of mild steel in the acidic media. Part I: gravimetric, electrochemical, SEM and XPS studies, Corros. Sci. 74, 271-282.
41. Guan N. M., Xueming L., & Fei L. (2004). Synergistic inhibition between O-phenanthroline and chloride ion on cold rolled steel corrosion in phosphoric acid, Mater Phys., 86, 59-68.
42. Abd-El-Rehim S. S., Refaey S. A. M., Taha F., Saleh M. B., & Ahmed R. A. (2001). Corrosion inhibition of mild steel in acidic medium using 2-aminothiophenol and 2-cyanomethylbenzothiazole, J. Electrochem Soc, 31, 429-435.
43. Chenette H. (1999). Chemical reactivity indexes in density functional theory, J. Comput. Chem. 20, 129-154.
44. Ebenso E. E., Arslan T., Kandemirli F., Caner N., & Love I. (2010). Theoretical studies on the corrosion performance of three amine derivatives on carbon steel: Molecular dynamics simulation and density functional theory approaches, Quant. Chem. 110, 1003-1018.
45. Musa A. Y., Kadhum A. H., Mohamad A. B., Rohoma A. B., & Mesmari H. (2010). Electrochemical and quantum chemical calculations on 4, 4-dimethyloxazolidine-2-thione as inhibitor for mild steel corrosion in hydrochloric acid, 969, 233-237.
46. Obot I. B., & Obi-Egbedi N. O. (2008). Fluconazole as an inhibitor for aluminium corrosion in 0.1 M HCl, Colloids and Surfaces A: Physicochemical and Engineering Aspects, 330 (2-3), 207-212.
47. Eddy N. O., Momoh-Yahaya H., & Oguzie E. E. (2015). Theoretical and experimental studies on the corrosion inhibition potentials of some purines for aluminium in 0.1M HCl, Journal of Advanced Research, 6(2), 203-217.
48. ObotI. B., & Obi-Egbedi N. O. (2008). Inhibitory effect and adsorption characteristics of 2, 3-diaminonaphtelene at aluminium/hydrochloric acid interface: Experimental and Theoretical study, Surface Review and Letters, 15(6), 903-910.
49. Döner A., Solmaz R., Özcan M., & KarasG. (2011). Experimental and Theoretical studies of Thiazoles as corrosion inhibitors for mild steel in sulphuric acid solution, Corrosion Science, 53 (9), 2902-2913.
50. Gece. G. (2008). The use of quantum chemical methods in corrosion inhibitors studies, Corros. Sci., 50, 2981-2992.
51. Khalil N. (2003). Quantum chemical approach of corrosion inhibition, Electrochemica Acta 48, 2635-2640.
52. Gomez B., Likhanova N. V., Dominguez-Aguilar M. A., Vela R., Martinez-Palou A., & Gasquaz J. (2006). Quantum chemical study of the inhibitive properties of 2-Pyridyl Azoles, J. Phys. Chem. B 110, 8928-8934.
53. Khaled K. F., Babic-Samardzija K., Hackerman N. (2005). Theoretical study of the structural effects of polymethylene amines on corrosion inhibition of iron in acid solutions, Electrochemica Acta 50, 2515-2520.
54. Bereket G., Hür E., & Ogretir C. (2002). Quantum chemical studies on some imidazole derivatives as corrosion inhibition for iron in acidic medium, Journal of Molecular Structure THEOCHEM, 578, 79-88.
55. Saranya J., Sounthari P, Paranswari K., & Chitra S. (2015). Adsorption and density functional theory on corrosion of mild steel by a quinoxaline derivative, Der Pharma Chemica, 7(8), 187-196.
56. Udhayakala P., Rajendiran T. V., & Gunasekaram S. (2012). Theoretical approach to the corrosion inhibition efficiency of some pyrimidine derivatives using DFT method, Journal of Computational method in Molecular Design, 2,1-15.

57. Obi-Egbedi N. O., Obot I. B., El-Khaiary M. I., Umoren S. A., & Ebenso E. E. (2011). Computational Simulation and Statistical Analysis on the Relationship between Corrosion Inhibition Efficiency and Molecular Structure of Some Phenanthroline Derivatives on Mild Steel Surface, Int. J. Electrochem. Sci. 6, 5649-5675.
58. Gece G., & Bilgiç S. (2009). Quantum chemical study of some cyclic nitrogen compounds as corrosion inhibited of steel in NaCl media, Corros. Sci., 51, 1876-1878.
59. de Souza F. & S., Spinelli A. (2009). Caffeic acid as a green corrosion inhibitor for mild steel, Corros. Sci., 51, 642-649.
60. Martinez S. (2003). Inhibitory mechanism of mimosa tannin using molecular modelling and substitutional adsorption isotherms, Mater. Chem. Phys., 77, 97-102.
61. Parr R. G., Szentpaly L., & Liu S. (1999). Electrophilicity index, J. Am. Chem. Soc., 121, 1922-1924.
62. Hohenberg P., & Kohn W. (1964). Inhomogeneous Electron gas, Phys. Rev., 136: B864-B871.